

The Measurement of the Light Deflection from Jupiter: Experimental Results

E. B. Fomalont

National Radio Astronomy Observatory, Charlottesville, VA 22903

efomalon@nrao.edu

S. M. Kopeikin

Dept. of Physics and Astronomy, University of Missouri-Columbia, Columbia, MO 65211

kopeikins@missouri.edu

ABSTRACT

We have determined the relativistic light deflection of the quasar J0842+1835 as Jupiter passed within $3.7'$ on 2002 September 8, by measuring the time delay using the VLBA and Effelsberg radio telescopes at 8.4 GHz. At closest approach, General Relativity (GR) predicts a radial (static) deflection of $1190 \mu\text{arcsec}$, and tangential (retarded or dynamic) deflection in the direction of Jupiter's motion of $51 \mu\text{arcsec}$. Our experiment achieved an rms position error of $\leq 10 \mu\text{arcsec}$, and measured this retarded deflection to be 0.98 ± 0.19 (rms error) times that predicted by GR. Comments on the interpretation of this experiment as a measurement of the speed of gravity are given. The increased positional accuracy for this VLBI phase referencing experiment was achieved by using two calibrator sources.

Subject headings: gravitation—quasars: individual (QSO J0842+1835)—relativity techniques: interferometric

1. The Gravitational Deflection of Radio Waves by Jupiter

Einstein solved the equation of light propagation in the field of a static body, and predicted the deflection of light at the limb of the Sun of $1.75''$ (Einstein 1916), and this relativistic deflection was measured for the first time in 1919 (Dyson, Eddington & Davidson 1920). The deflection prediction by Einstein was confirmed in a series of other experiments, the most precise of which was made with Very Long Baseline Interferometry (VLBI) (Lebach et al. 1995). Kopeikin (2001, 2003a,b) generalized the problem of light propagation in the gravitational field of an arbitrary moving object, and showed that the first order term of the deflection depends on the retarded position of the moving object as defined by the retarded solution of the Einstein wave equations (see also Will (2003)).

A once-in-a-decade configuration occurred on September 8, 2002 when Jupiter passed within $3.7'$ of the bright radio quasar J0842+1835. If Jupiter is at an angular distance θ from the quasar, the relativistic time delay, $\Delta(\tau_{l,m})$, between two radio telescopes, separated by a distance $\mathbf{B}_{l,m}$, is

$$\Delta(\tau_{l,m}) = -(1 + \gamma) \frac{2GM_J}{c^3 r_{mJ}} \times \left[\frac{\mathbf{n} \cdot \mathbf{B}_{l,m}}{\theta} + \frac{(1 + \delta)\mathbf{B}_{l,m} \cdot \mathbf{v}_J}{\theta^2 c} \right] \quad (1)$$

where γ is the parameter of the parameterized post-Newtonian (PPN) formalism (Will 1993), G is the gravitational constant, c is the speed of light, M_J is the mass of Jupiter, \mathbf{n} is the unit vector from Jupiter to the radio source in the plane of the sky, and r_{mJ} is the distance between Jupiter to the m th telescope. The first term in the brackets is the zeroth order (static) radial deflection term,

and the second term in brackets is the first order (retarded) deflection in the direction of velocity of Jupiter with respect to the barycenter of the solar system, \mathbf{v}_J , in the plane of the sky. The term δ represents a scale factor for the retarded deflection with $\delta = 0$ for GR. The association of δ with gravitational field parameters is discussed in §4.

The order of magnitude of the deflection prediction on September 8 for the 6000-km telescope separation is a delay of 115 psec (deflection of 1190 μ arcsec) for the radial term, and a delay of 4.8 psec (deflection of 51 μ arcsec) for the retarded term. Although $v_J/c \approx 4 \times 10^{-5}$, the additional factor of $1/\theta$ amplifies the retarded term so that it is 4% of the radial term¹. A previous close passage occurred in 1988 March 21 (Treuhhaft & Lowe 1991) the radial deflection term was measured to an accuracy $\approx 15\%$ in accordance with GR. With improvements over the years in VLBI techniques, sub-milliarcsecond positional accuracy were now attainable, and measurement of the retarded term was feasible.

2. The Experimental Strategy

The VLBI experiment to measure the deflection of light of the quasar J0842+1835 by Jupiter was conducted during five days, centered on September 8, 2002. The radio array consisted of eleven telescopes: ten 25-meter telescopes of the Very Long Baseline Array (VLBA), plus the 100-meter diameter telescope at Effelsberg, Germany. The observing frequency was 8.45 GHz and ten hours were used for observations on each of 2002 September 4, 7, 8, 9, 12.

An array measures the difference in arrival time, the delay, for a quasar signal to reach each of the telescopes. Using a widely spaced array, unprecedented positional accuracy can be obtained. However, this delay is contaminated by many effects, both internal to and external to each telescope system. To remove these effects, radio astronomers use the technique of *phase referencing* (alternating observations of two sources) whereby observations of one source (the calibrator) are used to determine the delay errors associated with the target source (Beasley & Conway 1995). If the switching time and source separation between

calibrator and target are less than the temporal/spatial variation scale sizes, the relative position between the two sources can be accurately measured. However, the propagation delay along the quasar paths through the ionosphere and troposphere may be so variable in time and angle, that even fast switching will not completely remove these propagation changes, and relative position accuracies $\leq 30 \mu$ arcsec are difficult to obtain even with VLBI techniques.

After several sets of test observations in early 2002 (Fomalont & Kopeikin 2002), we decided to sequentially observe J0842+1835 with two known nearby calibrators: J0839+1802, separated 0.82° in position angle -132° ; and J0854+2006 (=OJ287), separated by 3.36° in position angle 63° . The three sources lie on a nearly straight line, which was exploited in the calibration procedure. The observing sequence was identical for the 5 observing days: We cycled observations through the three sources in 5.5 min, with about 100 such cycles per day, a reasonable compromise between removing the temporal effects with obtaining good accuracy of the measured delay. This observational technique was an improved variant of that used for the solar bending experiments in 1974 and 1975 (Fomalont & Sramek 1976). The jovian magnetosphere also produced a radial deflection of the radio waves (directed inward to Jupiter) and this anomalous bending was of concern. However, calculations suggested that this bending would be significantly less than the retarded deflection term, and special observing techniques (observing at two frequencies simultaneously) would have reduced the sensitivity of the experiment to the gravitational bending. The magnetosphere bending is discussed in more detail below.

3. The Data Reduction

3.1. The Radio Interferometer Response

A radio interferometer measures the complex spatial coherence function of the electromagnetic radiation field $A_{l,m} e^{i2\pi\psi_{l,m}}$ at a frequency ν between two telescopes denoted by l and m . If the intercepted electromagnetic radiation field is dominated by a small-diameter radio source, then the response of the interferometer, denoted as the

¹The amplification is due to the time lag between present and retarded positions of Jupiter (Kopeikin 2001).

complex visibility function $V_{l,m} e^{i2\pi\phi_{l,m}}$, is

$$V_{l,m} e^{i2\pi\phi_{l,m}} = A_{l,m} e^{(i2\pi\psi_{l,m})} \hat{G}_l \hat{G}_m^* e^{\frac{i2\pi\nu}{c}(\Delta\tau_l - \Delta\tau_m)} \quad (2)$$

The complex gains of the telescopes, \hat{G}_l , contain the amplification and phase shifts that are introduced by each telescope system (* denotes complex conjugate), and the residual time delay (observed - model) of the signal from the radio source to each telescope is denoted by $\Delta\tau_l$. For an array of N telescopes, the visibility function is sampled simultaneously with $N(N - 1)/2$ interferometers, 55 pairs for an eleven-element array.

The accurate delay model was calculated using the Goddard Space Flight Center (GSFC) CALC software package version 9.1², which uses the most recent parameters associated with the earth rotation and orientation, nutation, the terrestrial reference frame, and the radio source positions defined on the celestial reference frame (Ma et al. 1998). We have slightly modified the CALC package to incorporate the gravitational deflection from all significant solar system bodies including the retardation term. We have assumed that the PPN parameter $\gamma = 1$, because it has been measured to 0.1% accuracy (Lebach et al. 1995) and we could not improve this value in our experiment. Additional delay variables during the experiment were monitored during the observations by making use of weather and ionospheric data available from GSFC data archives collected by Global Positioning Satellites.

The phase part of the complex visibility function (called simply the phase) for each source a , can be written as

$$\phi_{l,m}^a(t) = \frac{\nu}{c} \left[\mathbf{B}_{l,m} \cdot \Delta \mathbf{K}^a(t) + \Delta \mathbf{B}_{l,m}(t) \cdot \mathbf{K}^a + \Delta C_{l,m}(t) + \Delta A_{l,m}^a(t) \right] + \psi_{l,m}^a \quad (3)$$

where $\mathbf{B}_{l,m}$ is the model separation between telescope l and m , $\Delta \mathbf{B}_{l,m}(t)$ is the separation error; \mathbf{K}^a is the model position of the a th source, $\Delta \mathbf{K}^a(t)$ is the position offset error for the a th source, $\Delta C_{l,m}(t)$ is the residual clock delay between telescopes, and $\Delta A_{l,m}^a(t)$ is the residual tropospheric/ionospheric delay in the direction to a th

source. Higher order terms can be neglected since the a priori model and source positions are well-known. For this experiment, a has three values: $a = 0$ (J0842+1835), $a = 1$ (J0839+1802), $a = 2$ (J0854+2006). The occasional lobe ambiguities (arbitrary turns of phase) of the phase measurements were easily determined because of the accuracy of the delay model.

3.2. The Source Structure

The structures for each source on each day were determined from their respective complex visibility function using self-calibration techniques for radio imaging (Walker 1995). This imaging/deconvolution iteration process does *not* determine the accurate position of the sources, only their shapes. The derived images of the three quasars during the experiment are shown in Fig. 1. All three sources show the typical structure associated with most luminous radio sources, a bright component (core) at one end of the structure containing an appreciable part of the emission, and a more extended emission, often with a secondary bright component. There were no apparent change in the intensity and shape of the sources, except for a small change in J0854+2006 at the 1% level, which was not significant for the astrometric part of the experiment. The separation of the radio core and the secondary component for all sources was stable to $\leq 20 \mu\text{arcsec}$, an accuracy consistent with the sensitivity of the observations and the somewhat diffuse nature of the secondary peak. These properties are in agreement with previous observations of J0842 (sources names will be abbreviated) and J0839 which show little long term structure changes (Fey & Charlton 2000; Beasley et al. 2001), whereas J0854 is a known variable source. The change in the measured phase associated with the structure difference in J0854 between September 4 and 12 is less than 0.003 turn for any baseline changes, which is significantly small and can be ignored.

Some compact components ($< 50 \mu\text{arcsec}$) in radio sources vary intensity considerably over hour time-scales because of galactic scattering at distance of ≈ 300 pc. It is possible that such scattering also irregularly moves the component position. However, we detected no short-term variability in all three sources greater than 4% over hour periods sources, and conclude that the compact com-

²www.sgl.crestech.ca/IVS-Analysis/software_tools/calc_solve/datafiles.htm

ponents are not affected by interstellar scattering. However, we emphasize that such movement of the source position, if it existed, would be detected in this experiment.

3.3. Removing the Temporal and Spatial Phase Errors

With the removal of the source structure terms, the phase in Eq. (3) becomes circular among the telescopes; that is $\phi_{l,m} = \phi_{l,n} + \phi_{n,m}$, apart from stochastic noise. Therefore, there are only 10 independent phases for an array of 11-telescopes. We can thus chose a reference telescope, M , and write Eq. (3) for each source a and telescope l as

$$\phi_{l,M}^a(t) = f_{l,M}(t) + \mathbf{g}_{l,M}(t) \cdot (\mathbf{K}^a - \mathbf{K}^0) + \Delta \mathbf{K}^a(t) \cdot \mathbf{B}_{l,M} \quad (4)$$

where M is the reference telescope, and $f_{l,M}(t)$ is a function of time, dominated by the clock drifts. The term $\mathbf{g}_{l,M}(t)$ is a changing phase gradient in the plane of the sky near the position \mathbf{K}^0 . Such a gradient is a good approximation to the phase error associated with the uncertain position of a telescope $\Delta \mathbf{B}_{l,M}$, which includes earth rotation and orientation, nutation and similar small astrometric errors. Another gradient component is produced by the changing refractivity of the troposphere and ionosphere in the direction of the sources, from relatively large clouds and turbulent cells larger than about five degrees, moving over the telescopes. Small clouds produce residual errors in the measured phases which are not described by the simple phase gradient and produce rapid phase changes. The last term in Eq. (4) cannot be written as part of the first two terms since it depends on the position offset for each source from the assumed value, with no phase continuity in the sky. We used Mauna Kea (MK), HI as the reference telescope for most of the observations since this telescope is at a high site with generally good atmospheric conditions. For the first three hours of each day when the source elevation at MK was $< 20^\circ$, we used the the Los Alamos, NM telescope as the reference telescope.

Since J0842 and the two calibrators are nearly linear in the sky, and the variation of $f_{l,M}(t)$ and $\mathbf{g}_{l,M}(t)$ are relatively smooth over the observing cycle time of 5.5 minutes, we can sum the phases of the two calibrators with a weight proportional

to their inverse distance from J0842, to remove the temporal and spatial changes of the phase to first order. The calibrated phase for J0842, $\Phi_{l,M}$ for any day for telescope l becomes

$$\Phi_{l,M} = \phi_{l,M}^0 - (0.80\phi_{l,M}^1 + 0.20\phi_{l,M}^2) \approx \mathbf{B}_{l,M} \cdot (\Delta \mathbf{K}^0(t) - 0.80\Delta \mathbf{K}^1(t) - 0.20\Delta \mathbf{K}^2(t)) \quad (5)$$

If the two calibrators and target source are not linear in the sky, then a third calibrator must be observed in order to remove the spatial phase gradient from the target source.

Examples of the effectiveness of this calibration process is shown in Fig. 2 for the Owens Valley, CA to Mauna Kea, HI baseline on September 9. The observed phases, $\phi^a(t)$, (top plot) for the three sources follow each other over the day, but are separated at any time by an amount which is varying, caused by a phase wedge in the atmosphere. The displacement of phase between J0854 and J0842 is larger and in the opposite sense than that from J0839 and J0842, as expected from a wedge. The calibrated phase Φ of J0842, (bottom) is relatively smooth and near zero phase. The relatively small scatter is caused by fluctuations of phase shorter in temporal scale than about five minutes, or smaller in angular scale than five degrees. The signal to noise inherent in the observations cause only a small part of the scatter.

There are periods of time when the phase stability shown by all three sources noticeably deteriorates, and the calibrated phase of J0842 becomes large. These periods often occur when the source is at a low elevation, typically less than 20° , when large and non-linear tropospheric and ionospheric phase are more likely. Occasionally at high elevations during periods of rainy and windy conditions, VLBI observations are useless. These periods of obvious poor phase stability were removed from further consideration, and consisted of 15% of the original data. On the average the phase stability at sites with dry conditions was more stable than at those with humid conditions.

The calibrated phases, $\Phi_{l,M}(t)$, were then averaged for each day over a one hour period, with an estimated error determined from the scatter, which is about 0.02 turn per point. In Fig. 3, we show these averaged calibrated phases for two telescopes. The calibrated phases repeat extremely well from day to day to an accuracy of about 0.02

turns. Even a slight negative offset at $\text{GST} \approx 15$ hr repeats, and is produced by a ~ 50 μarcsec offset of the source positions from that assumed in the model, as given in Eq. (5).

3.4. The Deflection on September 8

The difference between the calibrated phase on September 8, and the average of the phases from the other days, is shown in Fig. 4 for the same two telescopes as in Fig. 3. Assuming that the position of all three sources remain fixed with respect to the *apriori* model, which includes the radial and retarded gravitational bending predicted by GR, the phases in Fig. 4 should scatter around zero phase, corresponding to $\delta = 0$. The curve given by $\delta = -1$ shows the expected calibrated phase on September 8 if the retarded deflection term were zero. Fig. 4 already demonstrates that $\delta \approx 0$, and that the experiment has clearly detected the retarded component of the light deflection.

An analysis of the effect of the jovian magnetosphere, has been described fully (Kopeikin & Fomalont 2002), and is summarized here. From measurements of the electron plasma density, N_0 , near the jovian surface made with the Galileo spacecraft, and an assumed spherically-shaped magnetosphere which decreases as $N_0(R_J/r)^{2+A}$, where $R_J = 7.1 \times 10^7$ m is the mean radius of Jupiter, we have integrating the estimated plasma delay at 8.45 GHz along the propagation path of J0842 at closest approach (3.7' or $13R_J$). We obtain magnetospheric deflection estimates of 17.5, 1.0, 0.02 μarcsec for $A = 0.0, 1.0, 2.0$, respectively. Based on the analogy with radial distribution of the solar corona, which suggests $A \approx 0.33$, we have determined the position shift associated with this jovian magnetosphere model (it is in the opposite direction of the gravitational radial deflection of light) and have shown its estimated phase contribution by the dashed line in Fig. 4. This estimate is probably substantially larger than the actual value on this day.

There are two ways in which we can combine the data in order to determine the mean gravitational deflection of J0842. First, we averaged the data for each telescope, and determined δ associated with each telescope, and these results are shown in Table 1, listed in decreasing order of accuracy. We find that the most accurate determinations are associated with telescopes in the south-

west USA, about 5000 km from MK, because they are located at places with relatively stable and dry atmosphere. Telescopes in more humid locations give poorer results. The Effelsberg telescope, however, was critical in the determination of the accurate structure of the radio sources. All telescope determinations are consistent with $\delta = 0$ when their estimated errors are considered.

Table 1
Telescope Solutions for δ

Telescope	Baseline to MK (km)	δ
Hancock, NH	7500	-0.02 ± 0.25
Los Alamos, NM	4970	-0.20 ± 0.34
Kitt Peak, AZ	4490	$+0.52 \pm 0.38$
Owens Valley, CA	4015	-0.45 ± 0.42
Pie Town, NM	4800	$+0.30 \pm 0.44$
Fort Davis, TX	5130	-0.09 ± 0.52
North Liberty, IA	6160	-0.37 ± 0.53
Brewster, WA	4400	$+0.14 \pm 0.62$
Saint Croix, VI	8610	-0.82 ± 0.85
Effelsberg, Germany	10300	$+1.94 \pm 1.60$
$< \delta >$		-0.02 ± 0.19

Another method of display is to image the calibrated phase data for all baselines, which are measured during any one-hour period. The location of the peak of the image is the position of J0842, and these positions are shown in Fig. 5. The east/west position of the source is more accurately determine than the north/south position since the array spans mostly in the east/west direction. The east/west positions clearly show that the retarded component of the light deflection has been detected, and is consistent with GR. The red line shows the estimate of a reasonable jovian magnetospheric refraction, and is much smaller than the retarded deflection, particularly in the east/west direction.

The average value of the data for the observations over September 8, regardless of how the data are averaged (by telescope or by image), is

$$\delta = -0.02 \pm 0.19 \quad 1\text{-}\sigma \text{ error}$$

The measured retarded deflection associated with the motion of Jupiter is, thus, in good agreement with the prediction of GR.

4. Discussion

4.1. The Measurement Results

The measurement of the retarded deflection component from the motion of Jupiter is a confirmation of General Relativity, now associated with a first-order term in v/c with respect to the static Shapiro time delay.

The use of two calibrators, on either side of J0842, improved the positional accuracy of this VLBI experiment by a factor of two to three compared with previous observations of this type. Because of the relative simplicity of the experimental concept as a classical deflection-type experiment, the uniform observational procedure over the entire experiment, the data redundancy provided by the number of telescopes and the number of days, we are convinced that the result and error estimate are accurate and demonstrated from the Fig. 4 and Fig. 5 which display a significant part of the data. The refraction from the jovian magnetosphere is at least as small as we have estimated, and any indication of anomalous bending caused by interstellar scattering is not seen since the scatter in Fig. 5 around the retarded curve is no larger than that expected from the errors derived from the scatter in the observations among all of the days.

The two-calibrator technique, developed in this experiment to remove the delay variations of the tropospheric-induced phase wedge above the telescopes, can be used for determinations of the proper motion and parallax of radio sources. With the relative positional sensitivity of $10 \mu\text{arcsec}$, the trigonometric parallax of stars and pulsars as far as 10 kpc can be determined; spacecraft can be tracked with an accuracy of 30 m near Jupiter; and the proper motion of radio sources in M31 can be determined to 5 km/sec over ten years.

4.2. The Measurement Interpretation

The main interpretation of this experiment is that the measurement of the retarded component of the gravitational bending from Jupiter is in good agreement with the prediction of General Relativity. If the question is asked: What gravitational parameter is most sensitive to this type of measurement, a physical significance must be attached to the δ parameter.

The analysis of the Jupiter deflection experi-

ment was described by Kopeikin (2001, 2003a,b). He developed a parameterized approach to the linearized Einstein-Maxwell equations by replacing in the Einstein equations the constant ‘speed of light’ parameter, c , explicitly with the ‘speed of gravity’ parameter, c_g , where appropriate. The integration of a light geodesic past a moving body gives the expression in Eq. (1) with the relationship, $\delta = (c/c_g) - 1$. Hence, our measured value of δ gives $c_g = (1.06 \pm 0.21) c$, in complete agreement with GR.

Will (1993, 2003) used the PPN formalism to determine the dependence of c_g for the Jupiter deflection experiment. He finds that the PPN parameters γ and α_1 appear in the VLBI time delay in the form, $\zeta = \alpha_1/(2 + 2\gamma)$, with no explicit dependence on c_g (see however (Kopeikin 2003b)). Assuming that $\gamma = 1$, we have determined $\alpha_1 = -0.1 \pm 0.8$ ($1-\sigma$) error. Although the value of α_1 measured from the laser ranging experiments (Müller, Nordtvedt & Vokrouhlický 1996) and the binary pulsar observations (Bell, Camilo & Damour 1996) gives considerably more stringent limits to α_1 under assumption that the preferred frame is known, our deflection experiment sets a limit on α_1 directly without additional assumptions. Further discussion of the results obtained by Will (2003) can be found in (Kopeikin 2003b).

In a recent paper Asada (2002) claimed that the velocity of Jupiter in Eq. (1) is a relative velocity with respect to an observer on earth. Our experimental result disproves this assertion.

What is perhaps more clear is that if this experiment had measured δ significantly different from zero (and this result was accepted!) then a problem would exist with the current formulation of GR and, as such, any interpretation of the result would be ambiguous and depend on the generalization of GR that was chosen. However, this measurement of the deflection of light by Jupiter is in good agreement with GR and demonstrates experimentally that the retarded position of Jupiter should be used in the determination of the deflection of light.

The National Radio Astronomy Observatory is a facility of the National Science Foundation, operated under cooperative agreement by Associated Universities, Inc. We thank the support from the Department of Physics and Astronomy of the Uni-

versity of Missouri-Columbia, and the Research Council of the University of Missouri-Columbia. The Max-Planck-Institut für Radioastronomie operates the Effelsberg 100-m Radio Telescope. We thank the VLBA staff for their help and support in obtaining and correlating the data. Support from the Eppley Foundation for Research (award #002672) is highly appreciated.

REFERENCES

Asada, H. ApJ, 574, L69

Beasley, A. J., Gordon, A. J., Peck, A. B., Petrov, L., MacMillan, D. S., Fomalont, E. B. & Ma, C. 2002, *Astrophys. J. Suppl.*, 141, 13

Bell, J. F., Camilo, F., & Damour, T. 1996, ApJ, 464, 857

Einstein, A. 1916, Ann. d. Phys., 49, 769

Beasley, A.J. & Conway, J.E. 1995, in ASP Conf. Ser. 82, Very Long Baseline Interferometry and the VLBA, ed. J.A. Zensus, P.J. Diamond & P.J. Napier (San Francisco: ASP) 328

Dyson, F. W., Eddington, A. S. & Davidson, C. 1920, *Phil. Trans. Roy. Soc. (London)*, 220A, 291

Fey, A.L & Charlot, P. 2000, *Astrophys. J. Suppl.*, 128, 17

Fomalont, E.B. 2002 & Kopeikin, S. M. 200 in: Proc. 6th European VLBI Network Symp., eds. E. Ros, R.W. Porcas, A.P. Lobanov & J.A. Zensus, (Bonn: MPIfR) 53

Fomalont, E.B. & Sramek, R.A. 1975, *Phys. Rev. Lett.* 36, 1475

Kopeikin, S.M. 2001, *Astrophys. J.*, 556, L1.

Kopeikin, S.M. 2003a, *Astrophys. J.* submitted

Kopeikin, S.M. 2003b, *Phys. Lett. A*, submitted

Kopeikin, S.M. and Fomalont, E.B. 2002, in: Proc. 6th European VLBI Network Symp., eds. E. Ros, R.W. Porcas, A.P. Lobanov & J.A. Zensus, (Bonn: MPIfR) 49

Lebach, D.E., Corey, B.E., Shapiro, I.I., Ratner, M.I., Webber, J.C., Rogers, A.E.E., Davis, J.L. and Herring, T.A. 1995, *Phys. Rev. Lett.*, 75, 1439

Ma, C., Arias, E.F., Eubanks, T.M., Fey, A.L., Gontier, A.-M., Jacobs, C.S., Sovers, O.J., Archinal, B.A., Charlot, P. 1998, *Astron. J.*, 116, 516

Müller, J., Nordtvedt, K., and Vokrouhlický, D., 1996, *Phys. Rev. D*, 54, R5927

Shapiro, I. I. 1964, *Phys. Rev. Lett.*, 13, 789

Treuhhaft, R. N. & Lowe, S. T. 1991, *Astron. J.*, 102, 1879

Walker, R. C. 1995, in ASP Conf. Ser. 82, Very Long Baseline Interferometry and the VLBA, ed. J.A. Zensus, P.J. Diamond & P.J. Napier (San Francisco: ASP) 247

Will, C. M. 1993, *Theory and Experiment in Gravitational Physics* (Cambridge: Cambridge University Press)

Will, C. M. 2003, Submitted to ApJ

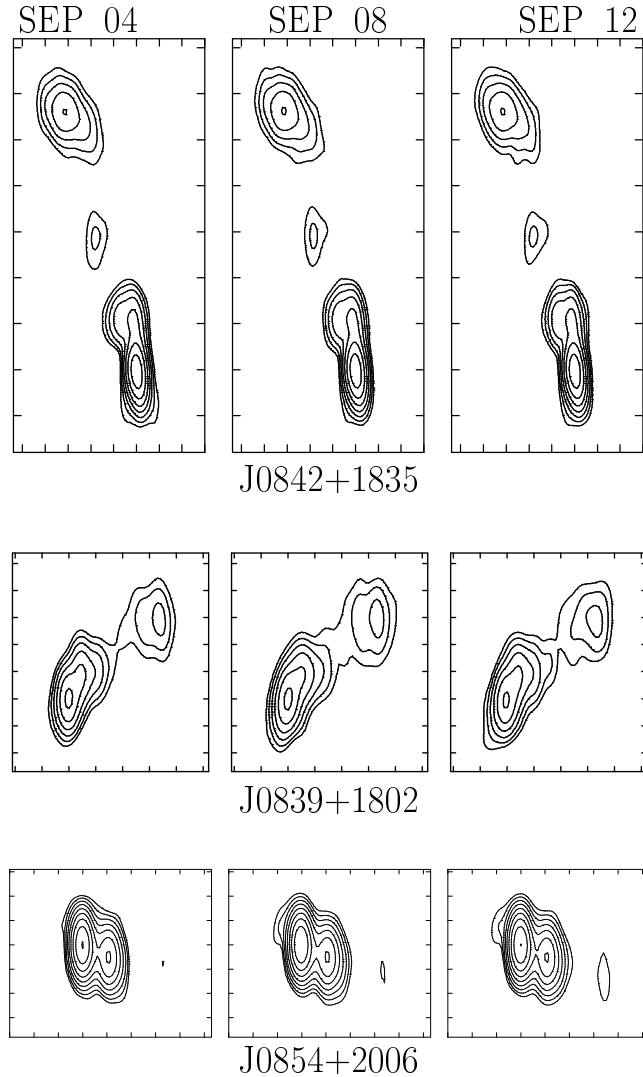


Fig. 1 - The Structure of the Three Quasars during the Experiment: The contour images for the three quasars on September 4, 8 and 12, are shown from left to right. The resolution is 1.5×1.0 mas, and the tick marks are separated by 1 mas (except for 2 mas the N/S axis of J0842+1835) and the lowest contour level is about 5 times the rms noise. The first row shows J0842+1835 with a lowest contour of 3.0 mJy/beam, about 1% of the peak brightnesses of 306.4, 308.5, 308.4 mJy/beam from left to right. The second row shows J0839+1802 with a lowest contour of 2.0 mJy/beam, about 2.8% of the peak brightnesses of 74.6, 75.5, 70.1 mJy/beam. The third row shows J0854+2006 with a lowest contour of 7.0 mJy, about 0.4% of the peak brightnesses of 1834, 1778, 1799 mJy/beam. The contour levels increase by a factor of two in brightness. The source J0854+2006 shows the emergence of a faint component to the east and a brightening of a weak component to the west.

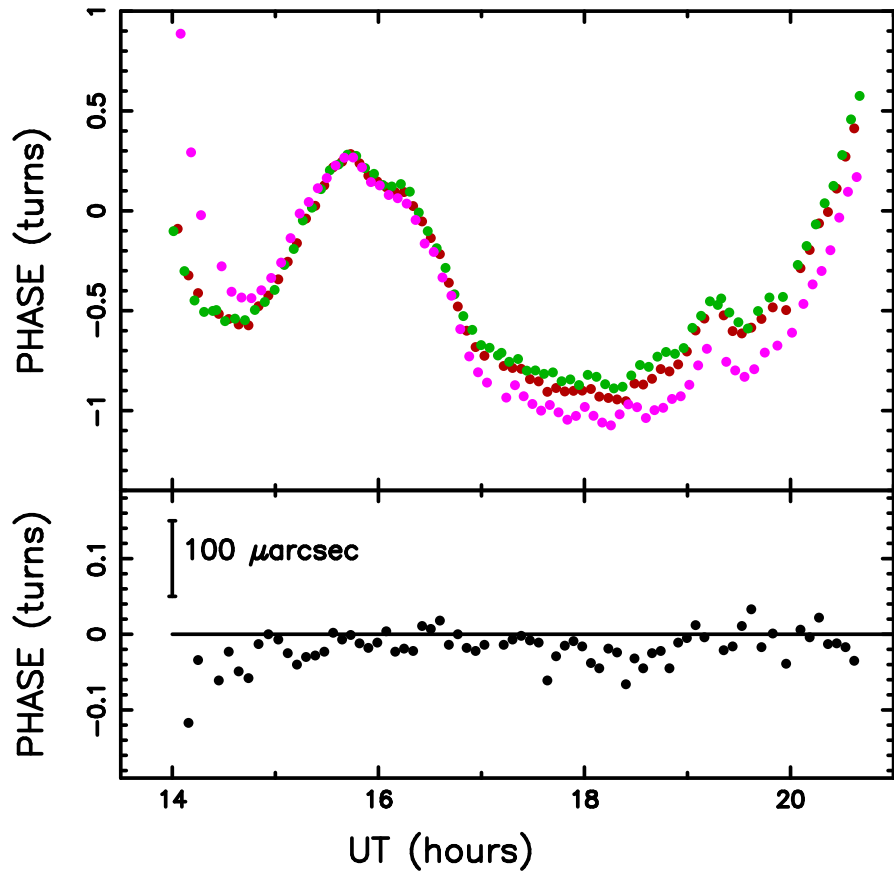


Fig. 2 - Removing the Residual Tropospheric and Ionospheric Delay Variations: The top plot shows the measured phase for the Owens Valley, CA to Mauna Kea, HI baseline on September 9 for each source. The red points are for J0842, the green points for J0839 and the purple points for J0854. The bottom plot shows the corrected phase for J0842 after using the linear interpolation of J0839 and J0854, defined by Eq. (5). The large phase gradient between UT 14h and 15h are produced by the low elevation of the sources and these data have been removed from further consideration.

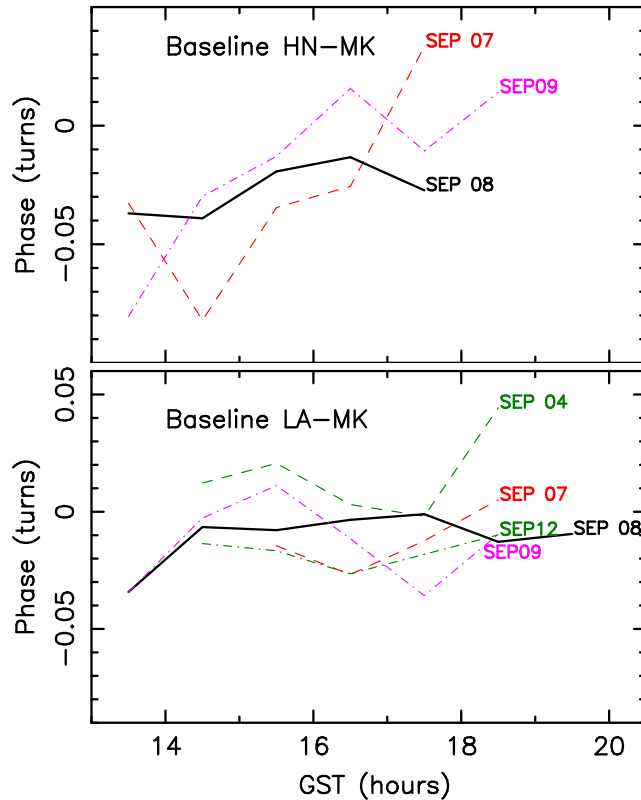


Fig. 3 - **The Calibrated Phases for the HN-MK and the LA-MK baselines for all Days.** The calibrated phases, averaged to one hour intervals on each day, for the Hancock, NH (top) and Los Alamos, NM (bottom) baselines to Mauna Kea, HI are connected by the line segments, with the day indicated at the right end of each line. The September 8 line is dark black. The error bars (not shown) are typically 0.02 turn per point. The Hancock telescope was not in use on Sep 4 and 12 because of telescope mechanical problems.

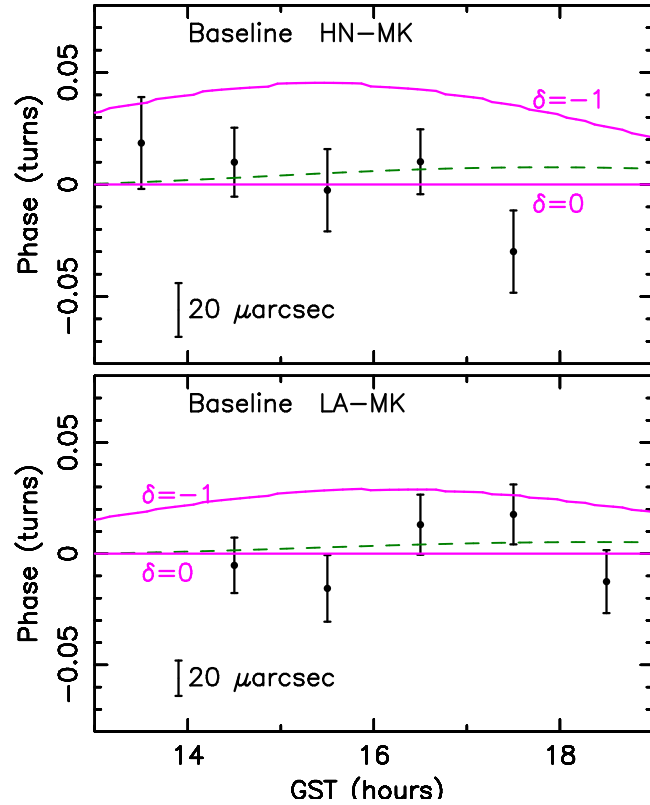


Fig. 4 - The Differential Calibrated Phase for September 8: The phase difference between the calibrated phase on September 8, and the average of that on the other days are given for Hancock (Top) and Los Alamos (Bottom) telescopes to Mauna Kea. The errors are derived from the scatter among the off-Jupiter days and the estimated error per point on September 8. The pink curve for $\delta = 0$ is that expected from GR; the blue curve for $\delta = -1$ is that expected for no retarded deflection component. The magnetosphere refraction estimate (see text) is shown by the dashed green line.

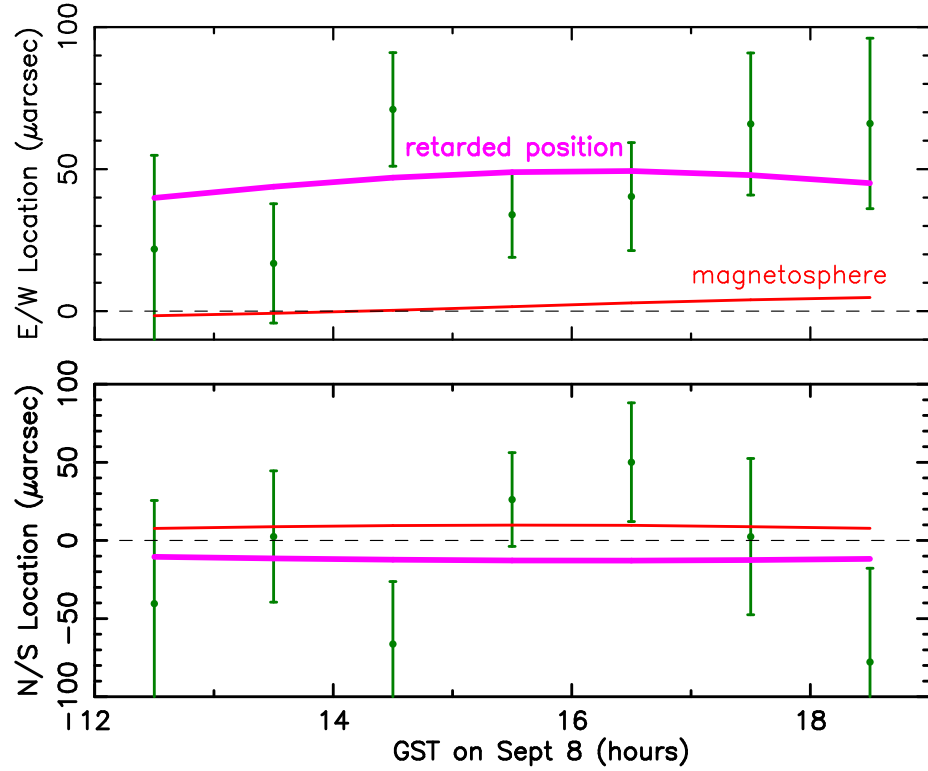


Fig. 5 - **The Retarded Deflection of J0842+1835 on September 8, 2002:** The plotted points and $1-\sigma$ error estimates show the retarded position every hour for J0842+1835; that is, the measured deflection in the direction of Jupiter's motion. The radial deflection term of $\approx 1200 \mu\text{arcsec}$ has been removed. The top plot shows the east/west position and the bottom plot shows the north/south position. The expected retarded deflection from GR ($\delta = 0$) is shown by the thick purple line. The estimated Jovian magnetosphere refraction is shown by the thin orange line.